Published in final edited form as:
Neuroscience. 2011 March 31; 178: 261–269. doi:10.1016/j.neuroscience.2011.01.021.

SELECTIVELY DIMINISHED CORPUS CALLOSUM FIBERS IN CONGENITAL CENTRAL HYPOVENTILATION SYNDROME

Rajesh Kumar[1], **Paul M. Macey**[2,3], **Mary A. Woo**[2], and **Ronald M. Harper**[1,3,*]
Dr. Miles Herkenham
Bethesda, MD, USA.

[1]Department of Neurobiology, David Geffen School of Medicine at UCLA, Los Angeles, CA 90095-1763, USA

[2]School of Nursing, University of California at Los Angeles, Los Angeles, CA 90095-1702, USA

[3]Brain Research Institute, University of California at Los Angeles, Los Angeles, CA 90095-1761, USA

Abstract

Congenital central hypoventilation syndrome (CCHS), a condition associated with mutations in the PHOX2B gene, is characterized by loss of breathing drive during sleep, insensitivity to CO_2 and O_2, and multiple somatomotor, autonomic, neuropsychological, and ophthalmologic deficits, including impaired intrinsic and extrinsic eye muscle control. Brain structural studies show injury in peri-callosal regions and the corpus callosum (CC), which has the potential to affect functions disturbed in the syndrome; however, the extent of CC injury in CCHS is unclear. Diffusion tensor imaging (DTI)-based fiber tractography procedures display fiber directional information and allow quantification of fiber integrity. We performed DTI in 13 CCHS children (age, 18.2±4.7 years; 8 male) and 31 control (17.4±4.9 years; 18 male) subjects using a 3.0-Tesla magnetic resonance imaging scanner; CC fibers were assessed globally and regionally with tractography procedures, and fiber counts and densities compared between groups using analysis-of-covariance (covariates; age and sex). Global CC evaluation showed reduced fiber counts and densities in CCHS over control subjects (CCHS vs controls; fiber-counts, 4490±854 vs 5232±777, $p<0.001$; fiber-density, 10.0±1.5 vs 10.8±0.9 fibers/mm^2, $p<0.020$), and regional examination revealed that these changes are localized to callosal axons projecting to prefrontal (217±47 vs 248±32, $p<0.005$), premotor (201±51 vs 241±47, $p<0.012$), parietal (179±64 vs 238±54, $p<0.002$), and occipital regions (363±46 vs 431±82, $p<0.004$). Corpus callosum fibers in CCHS are compromised in motor, cognitive, speech, and ophthalmologic regulatory areas. The mechanisms of fiber injury are unclear, but may result from hypoxia or perfusion deficits accompanying the syndrome, or from consequences of PHOX2B action.

Keywords

Cognition; Diffusion tensor imaging; Fiber tracking; Motor; White matter

[*]**Corresponding Author:** Ronald M. Harper, Ph.D. Department of Neurobiology David Geffen School of Medicine at UCLA University of California at Los Angeles Los Angeles, CA 90095-1763, USA rharper@ucla.edu Tel: 310-825-5303 Fax: 310-825-2224.

INTRODUCTION

Congenital central hypoventilation syndrome (CCHS), a disorder associated with mutations in the PHOX2B gene (Dauger et al., 2003, Stornetta et al., 2006, Dubreuil et al., 2008, Onimaru et al., 2008), is characterized by reduced drive to breathe during sleep, impaired sensitivity to CO_2 and O_2, and a range of autonomic, neuropsychological, cognitive, motor, and ophthalmologic deficits (Haddad et al., 1978, Paton et al., 1989, Goldberg and Ludwig, 1996, American Thoracic Society, 1999, Vanderlaan et al., 2004, Ruof et al., 2008). Brain structural studies in CCHS show gross white matter injury in multiple brain sites, including peri-callosal regions and the corpus callosum (CC) (Kumar et al., 2005, Kumar et al., 2006, Kumar et al., 2010); however, it is unclear whether localized CC fiber loss occurs, or whether the entire structure is compromised.

Injury either in cortical regions or their callosal fibers may contribute to deficits in the syndrome. The CC, the largest mass of white matter in the brain, projects fibers topographically between the hemispheres (de Lacoste et al., 1985, Hofer and Frahm, 2006), with defined areas containing fibers that serve cognitive, motor, speech, and vision functions (Darian-Smith et al., 1979, Moffat et al., 1998, Flannery et al., 2004, Caille et al., 2005, Narberhaus et al., 2008); CCHS subjects show impaired functions in all of these modalities (Goldberg and Ludwig, 1996, Vanderlaan et al., 2004, Ruof et al., 2008).

Assessment of microstructural changes within major fiber pathways requires techniques which can evaluate axons travelling in multiple directions. Non-invasive diffusion tensor imaging (DTI)-based fiber tractography procedures allow evaluation of individual fiber bundle integrity (Le Bihan et al., 2001, Eluvathingal et al., 2007); the technique reconstructs three-dimensional white matter trajectories using diffusion-weighted data by assessing directions of maximum water diffusivity represented by ellipsoid tensors (Conturo et al., 1999, Jones et al., 1999, Mori et al., 1999). Conventional magnetic resonance images or DTI indices possess no directional information, and thus, preclude detection of fiber pathways.

The purpose of this study was to examine global and regional fiber characteristics of the CC in CCHS and age- and sex-distributed control subjects. We hypothesized that CC fiber integrity is compromised in CCHS, reflected as diminished fiber counts and densities.

EXPERIMENTAL PROCEDURES

Subjects

We studied 13 CCHS (mean age ± SD: 18.2 ± 4.7 years; age range: 7−23 years; body-mass-index ± SD: 22.8 ± 6.1 kg/m^2; 8 male) and 31 control (17.4 ± 4.9 years; 7 −24 years; 21.8 ± 4.7 kg/m^2; 18 male) subjects. These CCHS and control subjects were used in one previously-published manuscript (Kumar et al., 2010), dealing with other issues; that earlier manuscript described different types of tissue injury (axonal vs myelin injury) in wide-spread brain areas in CCHS over control subjects. The CCHS diagnosis was based on guidelines of the American Thoracic Society (American Thoracic Society, 1999), and potential subjects were recruited through the CCHS family network (http://www.cchsnetwork.org). All CCHS subjects included in this study developed characteristics of the condition early in life. The range of respiratory impairments in CCHS varies from a need for continuous ventilatory support to support only during sleep; we included only those who required ventilatory support during sleep. Subjects with additional conditions that may contribute to brain injury, such as malnutrition (intestinal malabsorption or gut rotation issues), cardiovascular or neurological disorders, and Hirschsprung's disease, were also excluded.

All control subjects were in good health, without any history of neurological or other central nervous system-related disorders, and were recruited through advertisements at the university campus and neighbouring community. Control subjects with conditions inappropriate for a high-magnetic field environment, as indicated by the guidelines of the Institute for Magnetic Resonance Safety, Education, and Research (http://www.mrisafety.com/), were excluded from the study.

The study protocol was approved by the Institutional Review Board of the University of California at Los Angeles, and all subjects and their parents/guardians provided informed written consent/assent before the study. Personal identifiable information of all subjects was removed from the data evaluation records at completion of the analyses.

Magnetic resonance imaging

Brain studies of CCHS and control subjects were performed with a 3.0-Tesla magnetic resonance imaging scanner (Magnetom Tim-Trio; Siemens, Erlangen, Germany), using a receive-only 8-channel phased-array head-coil, and a whole-body transmitter coil. Foam pads were placed on both sides of the head to reduce head motion during scanning. High-resolution T1-weighted images were acquired using a magnetization prepared rapid acquisition gradient-echo pulse sequence (repetition-time = 2200 ms; echo-time = 2.34 ms; inversion time = 900 ms; flip angle = 9°; matrix size = 320×320; field-of-view = 230×230 mm; slice thickness = 0.9 mm; slices = 192). Proton-density and T2-weighted images were collected, covering the entire brain, using a dual-echo turbo spin-echo pulse sequence (repetition-time = 10,000 ms; echo-time 1, 2 = 12, 119 ms; flip angle = 130°; matrix size = 256×256; field-of-view = 230×230 mm; slice thickness = 3.5 mm; turbo factor = 5). Diffusion tensor imaging was performed using a single-shot echo-planar-imaging with a twice-refocused spin-echo pulse sequence (repetition-time = 10,000 ms; echo-time = 87 ms; flip angle = 90°; readout bandwidth = 1346 Hz/ pixel; matrix size = 128×128; field-of-view = 230×230 mm; slice thickness = 2.0 mm; no interslice-gap; diffusion gradient directions = 64; b = 0 and 700 s/mm^2). The generalized autocalibrating partially parallel acquisition parallel imaging technique, with an acceleration factor of two, was used for all brain scans.

Data processing

High-resolution T1-weighted, proton-density and T2-weighted images of CCHS and control subjects were visually examined to rule-out any subject with major anatomical defects, such as cysts, tumors, or any other mass lesions before data processing. Non-diffusion and diffusion-weighted images were also examined for any head motion-related or other imaging artifacts before data evaluation.

We used the Diffusion Toolkit (Version 0.5) and TrackVis (Version 0.5) (Wedeen et al., 2008), MRIcroN (Rorden et al., 2007), and MATLAB-based (The MathWorks Inc., Natick, MA) custom software for data evaluation.

Calculation of whole brain fiber tracks—The Diffusion Toolkit software was used to reconstruct DTI data and generate whole-brain fiber tracks. Diffusion tensors were calculated using the least-squares fitting method and eigenvalues, and eigenvectors were derived by standard procedures (Pierpaoli et al., 1996). Whole-brain fiber tracking was performed with the fiber assignment by a continuous tracking algorithm (Mori et al., 1999); the procedure allows seeding of tracks from entire brain voxels (Conturo et al., 1999). Instead of using a lower fractional anisotropy (FA) value, a whole-brain mask, derived from averaged diffusion-weighted images of individual subjects, with a minimum signal intensity was used to terminate fibers in non-brain regions in each subject. We used a 35° turning

angle between the principal eigenvectors of neighboring voxels to terminate tracking of fibers.

Corpus callosum fiber evaluation—We used MRIcroN to outline global CC regions of interest (ROI) and TrackVis software to visualize brain fibers and perform ROI analyses. Global and regional CC fiber tracks were examined in individual CCHS and control subjects. Using MRIcroN, the midline was identified in FA maps, and the entire CC outlined in the sagittal view in a single slice for each subject; all clusters within the CC were included in global CC ROI with FA values ≥ 0.45 (Fig. 1A, red). The global CC ROI was used to track fibers passing from the entire CC, and fiber tracks, with a minimum 10 mm fiber length, of individual subjects were counted. The fiber density of the global CC was calculated by fiber counts within the ROI area.

We used a mid-sagittal section of the CC to place ROIs. The CC was divided into six segments, prefrontal, premotor, sensorimotor, parietal, temporal, and occipital regions, using a suggested scheme of CC fiber organization across cortical brain regions (Pandya and Seltzer, 1986, Sullivan et al., 2006). In each segment of the CC, a spherical ROI with a radius of 1.5 mm was placed in native space of FA maps for fiber tracking (Fig. 1B), and fiber tracks of each ROI, with a minimum fiber length of 10 mm were counted.

Intra- and inter-tracker reliability and reproducibility

We established intra- and inter-tracker reliability for regional CC fiber evaluations; since global CC fiber evaluation was based on global CC ROI, derived from FA threshold, limiting chances for variability, inter- and intra-tracker reliabilities for global CC fiber tracking were not assessed. A principal investigator, who performed regional CC fiber tracking in all CCHS and control subjects, re-tracked fibers in 10 randomly-selected CCHS and control subjects. Another investigator also tracked fibers in the same subset of subjects with the same fiber tracking protocol. The mean fiber counts from repeated tracking of the primary and secondary investigators were calculated and compared with the initial findings of the primary investigator.

Statistical analyses

The Statistical Package for the Social Sciences (SPSS, V 18.0, Chicago, IL) software was used for statistical evaluation of the demographic data and fiber characteristics. Numerical demographic variables were assessed with an independent-samples t-test, and categorical values were evaluated with the Chi-square test. Global and regional CC fiber characteristics were evaluated with multivariate analysis of covariance, with age and sex included as covariates. Intra- and inter-tracker reliabilities were established with intraclass correlation (ICC) procedures. The mean fiber counts of different CC fiber bundles resulting from repeated time tracking with the primary investigator and with another investigator examining the same subject population were compared with paired t-tests for assessment of reproducibility. A p value less than 0.05 was considered statistically significant.

RESULTS

Demographics

No significant differences in age ($p = 0.60$), or body-mass-index ($p = 0.58$) appeared between the CCHS and control groups. Significant sex difference did not emerge between the groups ($p = 0.83$).

Corpus callosum fiber evaluation

The global CC fiber characteristics of CCHS and control subjects are summarized in Table 1, and individual fiber counts and density values are displayed in scatter plots (Fig. 2A, B). A substantial reduction in global CC fibers is visually evident in sample images of a CCHS and age- and sex-matched control subject (Fig. 3). The mean global fiber counts and densities were significantly reduced in CCHS compared to control subjects, controlling for age and sex (fiber counts, $p = 0.001$; fiber density, $p = 0.02$).

Regional CC fiber counts of CCHS and control subjects are summarized in Table 2, and individual values are displayed in scatter plots (Fig. 4). Multiple regions of CC showed reduced fiber counts in CCHS over control subjects, partitioning for age and sex, and these sites included regions within the CC that project to prefrontal, premotor, parietal, and occipital areas, compared to control subjects (prefrontal, $p = 0.005$; premotor, $p = 0.012$; parietal, $p = 0.002$; occipital, $p = 0.004$). A substantial regional reduction in CC fibers is visible in sample images from each group (Fig. 5).

Intra- and inter-tracker reliability and reproducibility

To determine intra- and inter-tracker reliability, a subset of 10 subjects was used, 3 were CCHS, and 7 were control subjects. Intra-tracker (prefrontal, ICC = 0.86, $p < 0.001$; premotor, ICC = 0.93, $p < 0.001$; sensori-motor, ICC = 0.86, $p < 0.001$; parietal, ICC = 0.90, $p < 0.001$; temporal, ICC = 0.93, $p < 0.001$; Occipital, ICC = 0.86, $p < 0.001$), as well as inter-tracker (prefrontal, ICC = 0.94, $p < 0.001$; premotor, ICC = 0.93, $p < 0.001$; sensori-motor, ICC = 0.91, $p < 0.001$; parietal, ICC = 0.93, $p < 0.001$; temporal, ICC = 0.85, $p < 0.001$; Occipital, ICC = 0.93, $p < 0.001$) reliabilities for all CC segments were significantly high.

No significant differences appeared between mean fiber counts from the first and second time-tracking by the primary investigator (first-pass vs second-pass; prefrontal, 260±34 vs 258±42, $p = 0.70$; premotor, 216±29 vs 213±28, $p = 0.40$; sensori-motor, 251±47 vs 245±40, $p = 0.44$; parietal, 217±65 vs 213±61, $p = 0.65$; temporal, 204±17 vs 204±15, $p = 0.72$; occipital, 425±56 vs 421±52, $p = 0.66$) and between first-time tracking by the primary and second investigator for all CC segments (primary investigator vs secondary investigator; prefrontal, 260±34 vs 260±34, $p = 0.84$; premotor, 216±29 vs 214±31, $p = 0.65$; sensori-motor, 251±47 vs 257±43, $p = 0.41$; parietal, 217±65 vs 216±52, $p = 0.83$; temporal, 204±17 vs 208±15, $p = 0.17$; occipital, 425±56 vs 424±52, $p = 0.92$), suggesting that measures of the fiber tracks were reproducible.

DISCUSSION

Overview

Global CC fiber counts and densities in CCHS were significantly reduced over control subjects, controlling for age and sex. These diminished fibers were localized within the CC in areas that project to prefrontal, premotor, parietal, and occipital regions. This study focused on using tractography procedures to outline interhemispheric characteristics of CC fibers. Other structural studies, including voxel-based T2-relaxometry and radial and axial diffusivity DTI procedures in CCHS subjects, show wide-spread injury to both myelin and axons in caudal and rostral brain areas, as well as in multiple sites within the CC (Kumar et al., 2005, Kumar et al., 2006, Kumar et al., 2008, Kumar et al., 2010). The affected CC fibers serve multiple brain functions, including cognitive, motor, and vision regulation (Darian-Smith et al., 1979, Flannery et al., 2004, Caille et al., 2005, Narberhaus et al., 2008), and CCHS subjects show such functional abnormalities (Goldberg and Ludwig, 1996, Vanderlaan et al., 2004, Ruof et al., 2008).

Reduced fiber counts: interpretation

In DTI-based fiber tractography procedures, fibers represent streamlines of voxels (series of connecting voxels) composing a particular fiber tract. The association between the streamlines of voxels and number of brain fibers has not been evaluated completely. The streamlines of voxels depend on the resolution of the DTI data and other parameters used in fiber assignment by continuous tracking algorithm-based fiber tracking procedures, including FA values and angular deflection thresholds for fiber termination. Since we used identical fiber tracking parameters, position, and size of the ROIs in CCHS and control subjects for regional CC evaluation, fiber counts of a specific site can be compared between groups, and any differences can be interpreted as loss of fiber integrity, resulting from microscopic white matter changes. Fiber counts are useful measures for evaluation of white matter injury in pediatric patients as are other DTI indices (Thomas et al., 2005).

Corpus callosum fiber characteristics

A reduction in global CC fiber counts and densities in CCHS subjects was more apparent after controlling for age and sex. The CC is heterogeneous in microstructure (Lamantia and Rakic, 1990), with areas containing both homotopically (symmetrical fiber connectivity between bilateral cortical areas) and heterotopically organized (asymmetrical fiber connectivity to functionally different cortical sites) fibers (de Lacoste et al., 1985, Pandya and Seltzer, 1986). The anterior- to posterior-organization of cortical sites is retained in the CC, with fibers originating in anterior and posterior areas of the cortex crossing in anterior and posterior portions of the CC, respectively. The CC contains large diameter fibers, which principally mediate sensorimotor coordination, and small diameter fibers that assist maintenance of excitation and inhibition between the cerebral hemispheres (Aboitiz et al., 1992a, b, Yazgan et al., 1995). Different cortical sites relay through different portions of the CC (Pandya and Seltzer, 1986). The large number of regulatory actions served by the CC include motor, speech, and vision control (Darian-Smith et al., 1979, Moffat et al., 1998, Flannery et al., 2004, Caille et al., 2005, Narberhaus et al., 2008), and involvement of the CC in cognitive regulation is well-known, based on patients with leukomalacia, children with an abnormal DS22q11.2 chromosome affecting callosal morphometry, callosal agenesis, as well as split-brain evidence (Gazzaniga and Smylie, 1984, Davatzikos et al., 2003, Badaruddin et al., 2007, Machado et al., 2007). In the current study, the overall fiber projections in CCHS and control subjects were well within the published descriptions in adults (Hofer and Frahm, 2006), although CCHS subjects showed reduced regional fibers. A reduction in global CC fibers may lead to inadequate recruitment of bilateral cortical sites, and introduce deficits in those associated functions.

Most CC subregions, including prefrontal, premotor, parietal, and occipital areas were affected; however, fibers serving the primary motor and temporal cortices were spared. In earlier studies, CCHS subjects showed injury in many areas, including prefrontal, premotor, parietal, and occipital cortices and surrounding fibers (Kumar et al., 2006, Kumar et al., 2010). The directional nature of fiber projections outlined here provides a more-complete description of fiber loss, and fiber injury in the CC subregion that projects to the occipital cortices shows extensive abnormality over earlier studies. Although seed points from previously-shown abnormal sites were not feasible due to technical limitations, we assessed CC areas in regions which normally project to those sites, and findings validate the earlier descriptions. The primary motor fibers of the pyramidal tract are relatively spared in CCHS (Kumar et al., 2008), except for lateral portions of the crus cerebri. Typically, gross motor behaviors are less affected in CCHS. Other fiber tracks in CCHS subjects show extensive injury, including fibers of the fornix (Kumar et al., 2009) and cerebellar-pontine fibers, based on preliminary observations.

Cognitive deficits and prefrontal fibers

Prefrontal CC fibers connect the left and right prefrontal cortices; the cortical region in one hemisphere serves to activate/suppress the analogous cortical area in the opposite hemisphere through these fibers (Hynd et al., 1995, Dorion et al., 2000). Damaged fibers would compromise interhemispheric communication between cortical sites, impairing site-specific functions.

The prefrontal cortex (PFC) serves multiple cognitive and executive actions, including working memory, behavioral inhibition, attention processing, and future planning (Barbey et al., 2009, Kadota et al., 2009, Prakash et al., 2009, Takahama et al., 2010). The site interconnects with a network which projects to, and receives projections from, cortical sensory, sub-cortical areas, and motor regions, including the caudate nuclei and putamen (Lehericy et al., 2004). Different types of cognitive processing are mediated across distinct sites of the PFC. The dorsomedial and lateral PFC, which receive auditory, visual, and somatosensory signals from temporal, occipital, and parietal areas, are linked with sensory and working or transient memory processing (Funahashi et al., 1989, Miller and Cohen, 2001). The medial PFC, which interacts with multiple limbic structures, is critical for cardiovascular control (King et al., 1999), memory, behavioral inhibition, and internal state processing, including motivation and affect (Miller and Cohen, 2001). The ventrolateral PFC regulates perceptual face and visual object stimuli processing, integrates mnemonic information from limbic structures, and maintains directed attention (Wilson et al., 1993, O Scalaidhe et al., 1997, Petrides, 2002). The dorsolateral PFC is associated with motor system structures, including supplementary and pre-supplementary motor areas, cerebellum, cingulate, and the superior colliculus (Miller and Cohen, 2001), and is implicated in reflexive behaviors and multiple working memory tasks (Pierrot-Deseilligny et al., 2003). Most of these sites, including the dorsomedial, medial, lateral, and ventrolateral PFC cortices, showed injuries in previous studies (Kumar et al., 2005, Kumar et al., 2006, Kumar et al., 2010), as well as fiber injury projecting to the sites described here.

CCHS subjects show several neuropsychological and developmental abnormalities that include cognitive, learning, and IQ deficits (Vanderlaan et al., 2004, Zelko et al., 2010). CCHS subjects show overall reduced mean group IQ values, but these values are exceptionally variable within ranges of the general population (Zelko et al., 2010). The cognitive issues in CCHS appear in working memory and attention, as well as social interaction (Vanderlaan et al., 2004, Ruof et al., 2008); these cognitive, as well as IQ deficits may partially develop from abnormalities of neuro-modulatory systems of the PFC. A prominent deficiency in CCHS is severely impaired autonomic regulation, manifested especially in cardiovascular control; part of such regulation stems from the medial PFC (King et al., 1999).

Motor and autonomic deficits and premotor fibers

CCHS subjects showed reduced premotor CC fibers, which are involved in motor coordination. Lesions in the CC interconnecting premotor and supplementary motor areas impair motor coordination, including bimanual coordination (Caille et al., 2005). Significant deficits in rhythm reproduction appear with injury in lateral or medial premotor cortex (Halsband et al., 1993), regions which interact with premotor fibers. Portions of the premotor areas include the “frontal eye fields,” which modify eye movements (Flannery et al., 2004). Stimulation of the cortical field on one side elicits conjugate eye movements directed to the other side (Flannery et al., 2004). Although detailed motor deficits in CCHS are not well described, subjects show both motor and speech developmental delays in addition to sleep-related suppression of respiratory motor action, and significant motor and eye coordination deficits (Goldberg and Ludwig, 1996, Vanderlaan et al., 2004).

As with the medial PFC, the loss of CC fibers which carry information from the insular cortices (Pandya and Seltzer, 1986) may interfere with autonomic regulation, heavily affected in CCHS (Woo et al., 1992, American Thoracic Society, 1999). The loss of fibers serving the insular cortices is especially important for both the parasympathetic and sympathetic components of the autonomic nervous system, since sympathetic regulation is preferentially mediated on the right and parasympathetic on the left insular cortex (Oppenheimer et al., 1992). Both insular cortices interact to maintain autonomic and cardiovascular stability. The propensity for sudden death in CCHS (Gronli et al., 2008) may stem from exaggerated or uncontrolled sympathetic output, unbalanced by parasympathetic action from ineffective fiber interactions.

Visuomotor coordination irregularities and parietal fibers

Corpus callosum fibers that project to parietal areas are significantly reduced in CCHS, compared to control subjects. Parietal areas contain sensory and motor cells, send and receive signals from frontal and supplementary motor areas (Fang et al., 2005), and are implicated in visuo-motor behavior and internal perception of oneself (Battaglia-Mayer et al., 2001, Breveglieri et al., 2006, Bakola et al., 2010). Patients with parietal injury show deficits in visual orientation, judgment of size and distance, localization of objects, manual reaching, and voluntary eye movements (Holmes, 1918); microelectrode studies show visual and somatic convergence in these areas (Hyvarinen et al., 1974). A principal complaint of CCHS subjects is the presence of visuo-motor coordination abnormalities (Goldberg and Ludwig, 1996); some of the deficits may result from the loss of fibers interconnecting the parietal cortices found here.

Ophthalmologic issues and occipital fibers

Corpus callosum fibers between the two occipital cortices are significantly reduced in CCHS subjects. The parieto-occipital region shows localized periventricular necrosis along with diffuse white matter gliosis in a case report of CCHS histopathology (Tomycz et al., 2010). The occipital portion of the corpus callosum projects to posterior visual areas, including the occipital and posterior parietal cortices, in a homotopic and heterotopic fashion (Putnam et al., 2009). These fibers are implicated in visual perception, as well as visual motor control for both intrinsic (parasympathetic fibers altering lens thickness for focusing, and sympathetic fibers regulating pupillary diameter), as well as extrinsic eye muscles (i.e., those used for eye movements). Asymmetric pupillary dilation is common in CCHS, as are complications related to eye movement; the majority of CCHS subjects show difficulties with reading, a complex visual task that incorporates complex eye scanning and movements, contrast and color perception, and eye focusing skills (Goldberg and Ludwig, 1996, Vanderlaan et al., 2004). Transfer of eye movement information between hemispheres, coordination of afferent and somatomotor information to autonomic outflow for focusing and adjustment to light levels, and compensation for depth perception are likely compromised in CCHS through the CC injury here, and manifested by a high incidence of strabismus and convergence insufficiency (Goldberg and Ludwig, 1996, Vanderlaan et al., 2004).

Potential mechanisms of fiber injury

Corpus callosum fiber injury may result from secondary effects of maldevelopment of cortical sites that give rise to CC fibers. Isolated areas of Phox2b expression in glia and fibers appear within cortical regions of mouse, and Phox2b heavily targets the locus coeruleus, source of adrenergic fibers to multiple cortical and other forebrain sites (http://www.gensat.org/index.html; http://developingmouse.brain-map.org/). It is unclear whether human PHOX2B effects are similarly distributed, but the locus coeruleus is heavily affected in isolated human cases (Tomycz et al., 2010), and shows structural injury in

grouped CCHS data (Kumar et al., 2006, 2008), as do pontine raphé regions responsible for serotonergic innervation over the neuraxis. Changes in both serotonergic and adrenergic innervation of cortical areas have the potential to exert significant cortical developmental consequences, with possible fiber loss. Similarly, fiber maldevelopment within the CC itself may result from mutation effects on fibers or on glia contributing to neuronal and fiber integrity. No Phox2b expression appears in the CC on any of the available murine atlases of Phox2b, suggesting that injury results from secondary effects of cortical neurons, from multiple hypoxic episodes accompanying CCHS, or from elevated carbon dioxide effects on glia.

Limitations

Several limitations should be considered in this study. Regional CC fiber characteristics were evaluated with manually-drawn ROI in individual subjects. Although special attention was paid to define ROIs in the same location of each CC segment in individual subjects, a possibility for slight variations in ROI location emerged. These findings should be considered to be accurate only within 2-3 millimeters.

Fiber tracking could have influenced separations of different fiber populations within a voxel (“kiss” or “cross” fibers); high-angular-resolution-diffusion-imaging DTI procedures may overcome this problem, as opposed to routine DTI techniques (Ozarslan and Mareci, 2003, Hess et al., 2006, Wahl et al., 2010). The procedures for high-angular-resolution-diffusion-imaging data require more diffusion directions, along with high diffusion-weighting (high b value). Although we had available 64 diffusion directions, which overcame this issue to some extent, scanner limitations restricted the potential to achieve higher diffusion-weighting.

CONCLUSIONS

Global CC fibers are reduced in CCHS compared to control subjects. Regional reductions of fibers appeared in areas of the CC that serve interhemispheric communication for prefrontal, premotor, parietal, and occipital cortex, which are implicated in motor, speech, cognition, and ophthalmologic regulation; aspects of visuomotor and intrinsic eye control, as well as planning are especially affected in CCHS. The primary motor and temporal CC fibers are relatively spared in the condition. The pathological mechanisms of CC fiber damage are unclear, but may result from developmental issues related to PHOX2B expression, or may be secondary to hypoxia and perfusion issues from hypoventilation in the condition.

Acknowledgments

Authors thank Ms. Rebecca Harper and Mr. Edwin M. Valladares for assistance with data collection, Drs. Jennifer Ogren and Heidi Richardson for scientific editing, and Ms. Alexa Chavez for assistance with data analyses. We thank CCHS subjects and their parents/guardians for their participation in this study. This research was supported by the National Institute of Child Health and Human Development R01 HD-22695.

ABBREVIATIONS

CCHS	Congenital central hypoventilation syndrome
CC	Corpus callosum
DTI	Diffusion tensor imaging
FA	Fractional anisotropy
ROI	Region of interest

PFC Pre frontal cortex

REFERENCES

Aboitiz F, Scheibel AB, Fisher RS, Zaidel E. Fiber composition of the human corpus callosum. Brain Res 1992a;598:143–153. [PubMed: 1486477]

Aboitiz F, Scheibel AB, Fisher RS, Zaidel E. Individual differences in brain asymmetries and fiber composition in the human corpus callosum. Brain Res 1992b;598:154–161. [PubMed: 1486478]

American Thoracic Society. Idiopathic congenital central hypoventilation syndrome: diagnosis and management. Am J Respir Crit Care Med 1999;160:368–373. [PubMed: 10390427]

Badaruddin DH, Andrews GL, Bolte S, Schilmoeller KJ, Schilmoeller G, Paul LK, Brown WS. Social and behavioral problems of children with agenesis of the corpus callosum. Child Psychiatry Hum Dev 2007;38:287–302. [PubMed: 17564831]

Bakola S, Gamberini M, Passarelli L, Fattori P, Galletti C. Cortical connections of parietal field PEc in the macaque: linking vision and somatic sensation for the control of limb action. Cereb Cortex 2010;20:2592–2604. [PubMed: 20176687]

Barbey AK, Krueger F, Grafman J. Structured event complexes in the medial prefrontal cortex support counterfactual representations for future planning. Philos Trans R Soc Lond B Biol Sci 2009;364:1291–1300. [PubMed: 19528010]

Battaglia-Mayer A, Ferraina S, Genovesio A, Marconi B, Squatrito S, Molinari M, Lacquaniti F, Caminiti R. Eye-hand coordination during reaching. II. An analysis of the relationships between visuomanual signals in parietal cortex and parieto-frontal association projections. Cereb Cortex 2001;11:528–544. [PubMed: 11375914]

Breveglieri R, Galletti C, Gamberini M, Passarelli L, Fattori P. Somatosensory cells in area PEc of macaque posterior parietal cortex. J Neurosci 2006;26:3679–3684. [PubMed: 16597722]

Caille S, Sauerwein HC, Schiavetto A, Villemure JG, Lassonde M. Sensory and motor interhemispheric integration after section of different portions of the anterior corpus callosum in nonepileptic patients. Neurosurgery 2005;57:50–59. [PubMed: 15987540]

Conturo TE, Lori NF, Cull TS, Akbudak E, Snyder AZ, Shimony JS, McKinstry RC, Burton H, Raichle ME. Tracking neuronal fiber pathways in the living human brain. Proc Natl Acad Sci U S A 1999;96:10422–10427. [PubMed: 10468624]

Darian-Smith I, Johnson KO, Goodwin AW. Posterior parietal cortex: relations of unit activity to sensorimotor function. Annu Rev Physiol 1979;41:141–157. [PubMed: 107850]

Dauger S, Pattyn A, Lofaso F, Gaultier C, Goridis C, Gallego J, Brunet JF. Phox2b controls the development of peripheral chemoreceptors and afferent visceral pathways. Development 2003;130:6635–6642. [PubMed: 14627719]

Davatzikos C, Barzi A, Lawrie T, Hoon AH Jr. Melhem ER. Correlation of corpus callosal morphometry with cognitive and motor function in periventricular leukomalacia. Neuropediatrics 2003;34:247–252. [PubMed: 14598230]

de Lacoste MC, Kirkpatrick JB, Ross ED. Topography of the human corpus callosum. J Neuropathol Exp Neurol 1985;44:578–591. [PubMed: 4056827]

Dorion AA, Chantome M, Hasboun D, Zouaoui A, Marsault C, Capron C, Duyme M. Hemispheric asymmetry and corpus callosum morphometry: a magnetic resonance imaging study. Neurosci Res 2000;36:9–13. [PubMed: 10678527]

Dubreuil V, Ramanantsoa N, Trochet D, Vaubourg V, Amiel J, Gallego J, Brunet JF, Goridis C. A human mutation in Phox2b causes lack of CO2 chemosensitivity, fatal central apnea, and specific loss of parafacial neurons. Proc Natl Acad Sci U S A 2008;105:1067–1072. [PubMed: 18198276]

Eluvathingal TJ, Hasan KM, Kramer L, Fletcher JM, Ewing-Cobbs L. Quantitative diffusion tensor tractography of association and projection fibers in normally developing children and adolescents. Cereb Cortex 2007;17:2760–2768. [PubMed: 17307759]

Fang PC, Stepniewska I, Kaas JH. Ipsilateral cortical connections of motor, premotor, frontal eye, and posterior parietal fields in a prosimian primate, Otolemur garnetti. J Comp Neurol 2005;490:305–333. [PubMed: 16082679]

Flannery T, Hewitt A, Choudhari KA. Isolated conjugate gaze palsy after frontal lobe tumour surgery. Br J Neurosurg 2004;18:627–629. [PubMed: 15799198]

Funahashi S, Bruce CJ, Goldman-Rakic PS. Mnemonic coding of visual space in the monkey's dorsolateral prefrontal cortex. J Neurophysiol 1989;61:331–349. [PubMed: 2918358]

Gazzaniga MS, Smylie CS. Dissociation of language and cognition. A psychological profile of two disconnected right hemispheres. Brain 1984;107:145–153. [PubMed: 6697151]

Goldberg DS, Ludwig IH. Congenital central hypoventilation syndrome: ocular findings in 37 children. J Pediatr Ophthalmol Strabismus 1996;33:175–180. [PubMed: 8771521]

Gronli JO, Santucci BA, Leurgans SE, Berry-Kravis EM, Weese-Mayer DE. Congenital central hypoventilation syndrome: PHOX2B genotype determines risk for sudden death. Pediatr Pulmonol 2008;43:77–86. [PubMed: 18041756]

Haddad GG, Mazza NM, Defendini R, Blanc WA, Driscoll JM, Epstein MA, Epstein RA, Mellins RB. Congenital failure of automatic control of ventilation, gastrointestinal motility and heart rate. Medicine 1978;57:517–526. [PubMed: 713831]

Halsband U, Ito N, Tanji J, Freund HJ. The role of premotor cortex and the supplementary motor area in the temporal control of movement in man. Brain 1993;116:243–266. [PubMed: 8453461]

Hess CP, Mukherjee P, Han ET, Xu D, Vigneron DB. Q-ball reconstruction of multimodal fiber orientations using the spherical harmonic basis. Magn Reson Med 2006;56:104–117. [PubMed: 16755539]

Hofer S, Frahm J. Topography of the human corpus callosum revisited--comprehensive fiber tractography using diffusion tensor magnetic resonance imaging. Neuroimage 2006;32:989–994. [PubMed: 16854598]

Holmes G. Disturbances of visual orientation. Br J Ophthalmol 1918;2:506–516. [PubMed: 18167823]

Hynd GW, Hall J, Novey ES, Eliopulos D, Black K, Gonzalez JJ, Edmonds JE, Riccio C, Cohen M. Dyslexia and corpus callosum morphology. Arch Neurol 1995;52:32–38. [PubMed: 7826273]

Hyvarinen, J.; Poranen, A.; Jokinen, Y. Central sensory activities between sensory input and motor output.. In: Schmidt, FO.; Worden, F., editors. The neurosciences: third study program. MIT Press; Cambridge, Mass: 1974. p. 311-317.

Jones DK, Simmons A, Williams SC, Horsfield MA. Non-invasive assessment of axonal fiber connectivity in the human brain via diffusion tensor MRI. Magn Reson Med 1999;42:37–41. [PubMed: 10398948]

Kadota H, Nakajima Y, Miyazaki M, Sekiguchi H, Kohno Y, Kansaku K. Anterior prefrontal cortex activities during the inhibition of stereotyped responses in a neuropsychological rock-paper-scissors task. Neurosci Lett 2009;453:1–5. [PubMed: 19429003]

King AB, Menon RS, Hachinski V, Cechetto DF. Human forebrain activation by visceral stimuli. J Comp Neurol 1999;413:572–582. [PubMed: 10495443]

Kumar R, Lee K, Macey PM, Woo MA, Harper RM. Mammillary body and fornix injury in congenital central hypoventilation syndrome. Pediatr Res 2009;66:429–434. [PubMed: 19581831]

Kumar R, Macey PM, Woo MA, Alger JR, Harper RM. Elevated mean diffusivity in widespread brain regions in congenital central hypoventilation syndrome. J Magn Reson Imaging 2006;24:1252–1258. [PubMed: 17075838]

Kumar R, Macey PM, Woo MA, Alger JR, Harper RM. Diffusion tensor imaging demonstrates brainstem and cerebellar abnormalities in congenital central hypoventilation syndrome. Pediatr Res 2008;64:275–280. [PubMed: 18458651]

Kumar R, Macey PM, Woo MA, Alger JR, Keens TG, Harper RM. Neuroanatomic deficits in congenital central hypoventilation syndrome. J Comp Neurol 2005;487:361–371. [PubMed: 15906312]

Kumar R, Macey PM, Woo MA, Harper RM. Rostral brain axonal injury in congenital central hypoventilation syndrome. J Neurosci Res 2010;88:2146–2154. [PubMed: 20209631]

Lamantia AS, Rakic P. Cytological and quantitative characteristics of four cerebral commissures in the rhesus monkey. J Comp Neurol 1990;291:520–537. [PubMed: 2329189]

Le Bihan D, Mangin JF, Poupon C, Clark CA, Pappata S, Molko N, Chabriat H. Diffusion tensor imaging: concepts and applications. J Magn Reson Imaging 2001;13:534–546. [PubMed: 11276097]

Lehericy S, Ducros M, Van de Moortele PF, Francois C, Thivard L, Poupon C, Swindale N, Ugurbil K, Kim DS. Diffusion tensor fiber tracking shows distinct corticostriatal circuits in humans. Ann Neurol 2004;55:522–529. [PubMed: 15048891]

Machado AM, Simon TJ, Nguyen V, McDonald-McGinn DM, Zackai EH, Gee JC. Corpus callosum morphology and ventricular size in chromosome 22q11.2 deletion syndrome. Brain Res 2007;1131:197–210. [PubMed: 17169351]

Miller EK, Cohen JD. An integrative theory of prefrontal cortex function. Annu Rev Neurosci 2001;24:167–202. [PubMed: 11283309]

Moffat SD, Hampson E, Lee DH. Morphology of the planum temporale and corpus callosum in left handers with evidence of left and right hemisphere speech representation. Brain 1998;121:2369–2379. [PubMed: 9874487]

Mori S, Crain BJ, Chacko VP, van Zijl PC. Three-dimensional tracking of axonal projections in the brain by magnetic resonance imaging. Ann Neurol 1999;45:265–269. [PubMed: 9989633]

Narberhaus A, Segarra D, Caldu X, Gimenez M, Pueyo R, Botet F, Junque C. Corpus callosum and prefrontal functions in adolescents with history of very preterm birth. Neuropsychologia 2008;46:111–116. [PubMed: 17897687]

Onimaru H, Ikeda K, Kawakami K. CO2-sensitive preinspiratory neurons of the parafacial respiratory group express Phox2b in the neonatal rat. J Neurosci 2008;28:12845–12850. [PubMed: 19036978]

Oppenheimer SM, Gelb A, Girvin JP, Hachinski VC. Cardiovascular effects of human insular cortex stimulation. Neurology 1992;42:1727–1732. [PubMed: 1513461]

Ozarslan E, Mareci TH. Generalized diffusion tensor imaging and analytical relationships between diffusion tensor imaging and high angular resolution diffusion imaging. Magn Reson Med 2003;50:955–965. [PubMed: 14587006]

Pandya, DN.; Seltzer, B. The topography of commissural fibers.. In: Lepore, F.; Ptito, M.; Jasper, HH., editors. Two hemispheres-one brain: functions of the corpus callosum. Alan R. Liss Inc.; New York: 1986. p. 47-74.

Paton JY, Swaminathan S, Sargent CW, Keens TG. Hypoxic and hypercapnic ventilatory responses in awake children with congenital central hypoventilation syndrome. Am Rev Respir Dis 1989;140:368–372. [PubMed: 2764373]

Petrides M. The mid-ventrolateral prefrontal cortex and active mnemonic retrieval. Neurobiol Learn Mem 2002;78:528–538. [PubMed: 12559832]

Pierpaoli C, Jezzard P, Basser PJ, Barnett A, Di Chiro G. Diffusion tensor MR imaging of the human brain. Radiology 1996;201:637–648. [PubMed: 8939209]

Pierrot-Deseilligny C, Muri RM, Ploner CJ, Gaymard B, Demeret S, Rivaud-Pechoux S. Decisional role of the dorsolateral prefrontal cortex in ocular motor behaviour. Brain 2003;126:1460–1473. [PubMed: 12764065]

Prakash RS, Erickson KI, Colcombe SJ, Kim JS, Voss MW, Kramer AF. Age-related differences in the involvement of the prefrontal cortex in attentional control. Brain Cogn 2009;71:328–335. [PubMed: 19699019]

Putnam MC, Steven MS, Doron KW, Riggall AC, Gazzaniga MS. Cortical projection topography of the human splenium: hemispheric asymmetry and individual differences. J Cogn Neurosci 2009;22:1662–1669. [PubMed: 19583478]

Rorden C, Karnath HO, Bonilha L. Improving lesion-symptom mapping. J Cogn Neurosci 2007;19:1081–1088. [PubMed: 17583985]

Ruof H, Hammer J, Tillmann B, Ghelfi D, Weber P. Neuropsychological, behavioral, and adaptive functioning of Swiss children with congenital central hypoventilation syndrome. J Child Neurol 2008;23:1254–1259. [PubMed: 18984833]

O Scalaidhe SP, Wilson FA, Goldman-Rakic PS. Areal segregation of face-processing neurons in prefrontal cortex. Science 1997;278:1135–1138. [PubMed: 9353197]

Stornetta RL, Moreira TS, Takakura AC, Kang BJ, Chang DA, West GH, Brunet JF, Mulkey DK, Bayliss DA, Guyenet PG. Expression of Phox2b by brainstem neurons involved in chemosensory integration in the adult rat. J Neurosci 2006;26:10305–10314. [PubMed: 17021186]

Sullivan EV, Adalsteinsson E, Pfefferbaum A. Selective age-related degradation of anterior callosal fiber bundles quantified in vivo with fiber tracking. Cereb Cortex 2006;16:1030–1039. [PubMed: 16207932]

Takahama S, Miyauchi S, Saiki J. Neural basis for dynamic updating of object representation in visual working memory. Neuroimage 2010;49:3394–3403. [PubMed: 19932754]

Thomas B, Eyssen M, Peeters R, Molenaers G, Van Hecke P, De Cock P, Sunaert S. Quantitative diffusion tensor imaging in cerebral palsy due to periventricular white matter injury. Brain 2005;128:2562–2577. [PubMed: 16049045]

Tomycz ND, Haynes RL, Schmidt EF, Ackerson K, Kinney HC. Novel neuropathologic findings in the Haddad syndrome. Acta Neuropathologica 2010;119:261–269. [PubMed: 19844731]

Vanderlaan M, Holbrook CR, Wang M, Tuell A, Gozal D. Epidemiologic survey of 196 patients with congenital central hypoventilation syndrome. Pediatr Pulmonol 2004;37:217–229. [PubMed: 14966815]

Wahl M, Barkovich AJ, Mukherjee P. Diffusion imaging and tractography of congenital brain malformations. Pediatr Radiol 2010;40:59–67. [PubMed: 19937239]

Wedeen VJ, Wang RP, Schmahmann JD, Benner T, Tseng WY, Dai G, Pandya DN, Hagmann P, D'Arceuil H, de Crespigny AJ. Diffusion spectrum magnetic resonance imaging (DSI) tractography of crossing fibers. Neuroimage 2008;41:1267–1277. [PubMed: 18495497]

Wilson FA, Scalaidhe SP, Goldman-Rakic PS. Dissociation of object and spatial processing domains in primate prefrontal cortex. Science 1993;260:1955–1958. [PubMed: 8316836]

Woo MS, Woo MA, Gozal D, Jansen MT, Keens TG, Harper RM. Heart rate variability in congenital central hypoventilation syndrome. Pediatr Res 1992;31:291–296. [PubMed: 1561018]

Yazgan MY, Wexler BE, Kinsbourne M, Peterson B, Leckman JF. Functional significance of individual variations in callosal area. Neuropsychologia 1995;33:769–779. [PubMed: 7675166]

Zelko FA, Nelson MN, Leurgans SE, Berry-Kravis EM, Weese-Mayer DE. Congenital central hypoventilation syndrome: neurocognitive functioning in school age children. Pediatr Pulmonol 2010;45:92–98. [PubMed: 19960523]

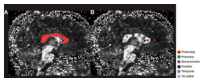

Figure 1.

Mid-sagittal view of fractional anisotropy maps with overlapped global and regional CC regions-of-interest. The left fractional anisotropy map (A) shows the global CC ROI (red), and the right fractional anisotropy map (B) shows regional ROIs of each CC segment. The colored circles, shown on different segments of the CC, are used for different CC fiber bundle assessment.

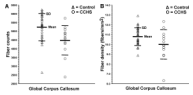

Figure 2.
Global CC fiber counts (A) and density values (B) from individual control (Δ) and CCHS (O) subjects. Both fiber counts and density values are significantly reduced in CCHS compared to control subjects, controlling for age and sex.

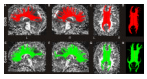

Figure 3.
Global CC fiber tracks and density in a CCHS and control subject. The upper panel shows left-side global CC fibers in a sagittal view (A), right-side fibers in sagittal view (B), and overall axial view of CC fibers, with (C) fractional anisotropy (FA) map in a CCHS subject (age, 22.6 years; female). The lower panel displays global left (E) and right-side (F) CC fibers in sagittal views, and overall view of those fibers with (G) background FA map in a control subject (age, 22.4 years; female). For better visualization of these fibers, images without background FA maps are displayed in the upper (D) and lower (H) panels. Overall, the CCHS subject showed reduced numbers and density of CC fibers relative to the control subject (CCHS vs. Control; fibers, 3990 vs. 4358; fiber density, 9.5 vs. 11.4 per mm^2). (*L* = Left; *R* = Right)

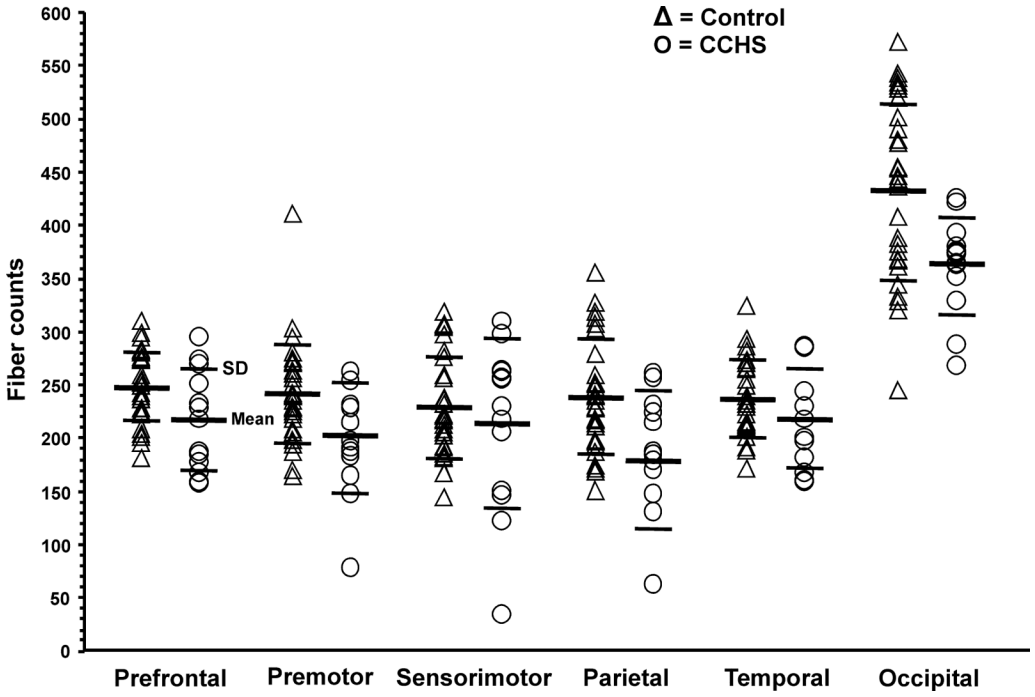

Figure 4.

Regional CC fiber count values from individual control (Δ) and CCHS (O) subjects. The CC sites that project to prefrontal, premotor, parietal, and occipital areas show reduced fiber counts in CCHS over control subjects, accounting for age and sex.

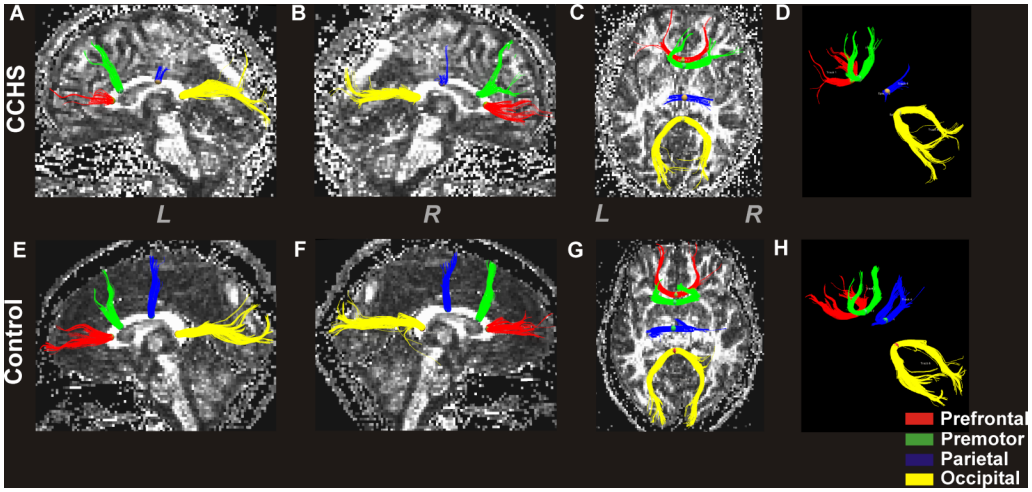

Figure 5.

Regional CC fiber tracks in a CCHS and control subject. The top panel shows left (A) and right-side (B) regional CC fibers that pass through a defined ROI in sagittal views, an overall view of fibers from the top in axial section (C) with a background fractional anisotropy (FA) map in a CCHS subject (age, 18.5 years; female). The lower panel shows left (E) and right-side (F) regional fibers in sagittal views, an overall view from above in axial section (G) with a background FA map in a control subject (age, 18.4 years; female). Images without background FA maps are also shown in upper (D) and lower (H) panels for better visualization of fibers. The CC regions that interconnect prefrontal, premotor, parietal, and occipital areas show reduced fibers in CCHS compared to the control subject (CCHS vs. control; prefrontal, 188 vs. 259; premotor, 166 vs. 251; parietal, 64 vs. 211; occipital, 374 vs. 437). (*L* = Left; *R* = Right)

Table 1

Global CC fiber characteristics of CCHS and control subjects.

Parameters	CCHS (n = 13) (mean ± SD) [A]	Controls (n = 31) (mean ± SD) [B]	*p values [A] vs [B]
GCC ROI area (mm^2)	449.6 ± 67.3	485.3 ± 83.6	0.102
Fiber counts	4490 ± 854	5232 ± 777	0.001
Fiber density (fibers/mm^2)	10.0 ± 1.5	10.8 ± 0.9	0.020

SD = Standard deviation; GCC = Global corpus callosum

* = p values derived from multivariate analysis of covariance, with age and sex included as covariates.

Table 2

Regional CC fiber counts of CCHS and control subjects.

CC segments	CCHS (n =13) (mean ± SD) [A]	Controls (n = 31) (mean ± SD) [B]	*p values [A] vs [B]
Prefrontal	217 ± 47	248 ± 32	0.005
Premotor	201 ± 51	241 ± 47	0.012
Sensorimotor	213 ± 79	229 ± 48	0.254
Parietal	179 ± 64	238 ± 54	0.002
Temporal	218 ± 47	236 ± 36	0.205
Occipital	363 ± 46	431 ± 82	0.004

CC = Corpus callosum; SD = Standard deviation

* = p values derived from multivariate analysis of covariance, with age and sex included as covariates.